NONLINEAR AND DISTRIBUTED PARAMETER MODELS OF THE MINI-MAST TRUSS

Lawrence W. Taylor, Jr.
NASA Langley Research Center
Hampton, VA

3rd NASA/DOD
Controls-Structures Interaction
Technology Conference
January 30, 1989

PRECEDING PAGE BLANK NOT FILMED

ABSTRACT

Large spacecraft such as Space Station Freedom employ large trusses in their construction. The structural dynamics of such trusses often exhibit nonlinear behavior and little damping which can impact significantly the performance of control systems. The Mini-MAST truss was constructed to research such structural dynamics and control systems. The Mini-MAST truss is an object of study for the Guest Investigator Program as part of NASA's Controls-Structures Interaction Program. The Mini-MAST truss is deployable and about 65 feet long. Although the bending characteristics of the Mini-MAST truss are essentially linear, the angular deflection under torsional loading has exhibited significant hysteresis and nonlinear stiffness. It is the purpose of this study to develop nonlinear and distributed parameter models of the truss and to compare the model dynamics with actual measurements. Distributed parameter models have the advantage of requiring fewer model parameters. A tangent function is used to describe the nonlinear stiffness in torsion, partly because of the convenience of its easily expressed inverse. Hysteretic slip elements are introduced and extended to a continuum to account for the observed hysteresis in torsion. The contribution of slipping to the structural damping is analyzed and found to be strongly dependent on the applied loads. Because of the many factors which affect the damping and stiffness in a truss, it is risky to assume linearity.

INTRODUCTION

Future missions in space require spacecraft which are considerably larger and more flexible than current spacecraft. Large spacecraft such as Space Station Freedom employ large, complex trusses in their construction. The structural dynamics of such trusses often exhibit nonlinear behavior and low structural damping which can impact significantly the performance of control systems. For example, in reference 1, Lallman studies the effect of damping on the performance of the attitude control system of the Space Station Freedom. The Mini-MAST truss was constructed to research the interaction of such structural dynamics and control systems and is an object of study for the Guest Investigator Program as part of NASA's Controls-Structures Interaction Program.

The Mini-MAST truss was designed to be deployable to a length of 66.14 feet when fully extended. The bending characteristics of the Mini-MAST truss are essentially linear. The angular deflection under torsional loading, however, has exhibited significant hysteresis and nonlinear stiffness during laboratory tests.

The complexity of such structures creates a burden to optimal design and to systems identification for upgrading dynamic model parameters by analyzing experimental test data. The large number of model parameters which results if each structural mode is assumed to be independent can be greatly reduced if distributed parameter models are used.

It is the purpose of this study to develop distributed parameter models of the Mini-MAST truss and to compare the model dynamics with the actual dynamic characteristics. A second purpose is to model the nonlinear stiffness and damping properties of this joint-dominated truss. It is hoped that the study results will be useful in designing control systems for large spacecraft (such as Space Station Freedom) which employ similar trusses.

DISCUSSION

Because the Mini-MAST truss is representative of structures that will be used for large spacecraft such as the Space Station Freedom, the study of its structural dynamics is valuable in assuring the dependability and high performance of spacecraft control systems. Figure 1a. pictures the Mini-MAST truss being deployed. The reduction in volume is striking when compared to the deployed truss shown in figure 1b. Reference 2 describes in detail the design of the Mini-MAST. Because of the complexity of the truss it is important to study simplifying models of its dynamics. Figure 2 shows how many modes are required to depict accurately the static deflection of a cantilevered beam. The problem is compounded if the modal parameters are considered to be independent. Because of the resulting complexity there is considerable advantage in using distributed parameter models. Due to the greatly reduced numbers of parameters required for such models as shown in figure 3, the ability to employ systems identification (Reference 3) and optimal design techniques is greatly facilitated. Because of these advantages it is valuable to determine the accuracy with which distributed parameter models can represent the Mini-

MAST truss. For example, can such simple models predict accurately the peaks of the frequency response shown in figure 4? If distributed parameter models represent accurately the dynamics of the Mini-MAST truss, then the model equations can be used to upgrade the model parameters using systems identification. Also the models will be useful in integrated control-structures design because their form provides easy access to global varibles such as the modulus of elasticity.

The Mini-MAST truss, being deployable, requires a large number of joints. The compliance and possible slippage of the joints may affect the overall stiffness of the truss when viewed as an equivalent beam. The action of the joints may also affect the damping of the truss as well. It is important to know accurately the damping of a spacecraft in order to assure reliable and high performance control. It is also important to understand and to model any nonlinear behavior caused by the numerous joints.

Distributed Parameter Bending Model

The Mini-MAST truss is modeled as a cantilevered beam with an added tip mass as depicted in the schematic in figure 5. The partial differential equations (Euler beam equation) and boundary condition equations (Cantilevered and tip mass) are solved thereby determining the modal characteristics. First, the calculated static deformation resulting from a constant 15 pound for applied to the tip is compared to actual test results in figure 6. The value of the stiffness parameter, EI, for an equivalent Euler beam derived from this test is 27.6×10^6 pound feet squared. The comparison suggests that the model deformation matches the actual deformation within the measurement error. The resulting modal frequencies in bending are then compared with experimental results and those for a finite element model* in figure 7. The frequencies for the first few bending modes of the distributed parameter model accurately match the actual bending frequencies of the truss. At higher mode numbers, however, the actual modal frequencies are lower than the theoretical values for the Euler beam model. Belvin** showed that the shear deformation of a similar truss cannot be ignored as is done in

***Bailey, James, Finite-Element Model of the Mini-MAST Truss, personal communication, NASA Langley.**

****Belvin, W. Keith, Simplified Analysis of NASA's COFS 1 MAST-Beam, personal communication, NASA Langley.**

the Euler beam model. Belvin used the techniques of reference 6 in his study. The Timoshenko beam, in contrast, accounts for the shear deformation and more accurately models the frequencies in bending as shown in figure 7.

Figure 7 also shows the accuracy with which the frequencies of a finite element model match the actual frequencies of the truss. The finite element model is reasonably accurate even at high mode numbers. The parameter, EI, used in the finite element model equals 29.8 x 10^6 pound feet squared. In figure 8 the bending mode shapes generated by the same finite element model exhibit shapes similar to Euler beams with one exception. Examination of the third mode reveals that the shear deformation is significant enough to give a change in slope almost at the bottom of the truss. The general contour of the mode shapes in figure 8 compare well with those of the Timoshenko beam (not shown) but the irregularities which show significant local deformation will be missing from the distributed parameter models. It is possible that overlookong such local deformations could cause control system instability.

The effect on the first bending mode frequency of changing the mass at the tip of the equivalent beam is shown in figure 9. The frequency response measurements of figure 4 had a tip mass which weighs 70.125 pounds (mass ratio = .31). The Mini-MAST truss excluding its tip mass weighs 229 pounds. The Euler beam model depicts accurately the change in frequency when the tip mass is removed. The assembly for the active control of the Mini-MAST is expected to weigh in excess of 300 pounds. The frequencies for higher mode numbers will not change as much as that for the first mode because as mode number increases the motion of the tip mass diminishes, thereby approaching a pinned end condition.

Distributed Parameter Torsion Model

Similar to the bending case, the truss is modeled in torsion as a uniform shaft which is fixed at one end and has a tip body attached to the other end. Based on the angular deformation due to an applied moment the torsional parameter GI_{polar} equals 2.16 x 10^6 pound feet squared per radian. The partial differential equations and end conditions are solved and in figure 10 the model's torsional frequencies are compared with experimental results and the finite element model of Bailey's personal communication. The close comparison indicates that the modal frequencies for both the distributed parameter model and the finite element model compare closely with the actual frequencies.

Nonlinear Torsional Stiffness

Because the Mini-MAST truss exhibits significant nonlinear stiffness and hysteretic behavior in torsion, it is necessary to model these characteristics. The nonlinear stiffness model will be discussed first. The hysteretic model will be treated in the next section.

Although the form of the nonlinear stiffness is approximately cubic, a tangent function is used because (1) its form gives the nearly linear plus cubic relationship that is needed, and (2) the tangent has a conveniently express inverse. Figure 11 depicts the tangent model of the nonlinear stiffness in torsion and introduces the parameters, K, and, B, which govern the linear and the cubic contribution, respectively. The parameter, K, then is the usual torsional stiffness.

In figure 12 it is evident that the tangent relationship compares well with the experimental results. The data shown are believed to not involve any slipping as it represents the relaxation from a load having been applied. As the load is increased slipping does take place and will next be considered.

Torsional Slip Model

The torsional hysteretic model is comprised of an infinite number of slip elements. An individual slip element is assumed to slip instantaneously upon reaching a particular moment threshold. A reverse slip is assumed to take place at a moment of equal level but opposite sign as depicted in figure 13. A slip distribution function is introduced which describes the probability density function of the values of moment threshold. The second order exponential form of the function, shown in figure 14, was chosen to fit the experimental data. Effort is under way to link this distribution function to the vertical loading of the joints. The total deflection amplitude consists of (1) the deflection due to compliance without slipping plus and (2) the deflection due to an accumulation of slips due to the applied moment. The expected value of the accumulation of slips is given by the integral of the slip distribution function between the last moment reversal or zero and the current applied moment. The deflection equation is depicted in figure 15.

The total hysteretic model which contains both the nonlinear stiffness and the hysteretic slipping is compared with actual test results in figure 16. The close comparison of the model results and the actual hysteretic behavior gives validity to the model for torsional deflection due to applied moment.

The hysteretic behavior is expected to be dependent on the vertical loading. When the 300 pound plus active control assembly is attached to the top of the Mini-MAST the total angular deflections are not expected to change significantly, but an increase in the moment threshold is expected. Because of the effect of gravity it is difficult to determine the hysteretic behavior in an unloaded condition as in space.

Structural Damping

The damping for the first bending mode is affected by the mass of the tip body as shown in figure 17. The damping ratio which was measured for the truss without tip mass was about 3.3%. This value was about three time the value expected based on the assumption that the dimensional damping of the truss would not change. The damping ratio would be expected to double from the value of about .45% for the 70 pound tip mass. This discrepancy is probably due to slipping being affected by vertical loading, as is the case for torsion.

In torsion it is possible to link slipping to damping by accounting for the loss of energy due to slipping. Figure 18 shows that the expected contribution to damping from slipping for oscillations about the unloaded condition reflect the shape of the slip distribution function. The damping contribution for oscillations in torsion about a loaded condition may be as low as zero because of the complete lack of slipping.

The statically determinant truss to be used on the Space Station Freedom can be expected to involve internal loading. As a result the damping of the truss for small amplitudes is not expected to involve slipping and will consequently exhibit very low damping.

Laboratory tests have revealed a damping ratio for bending modes for the cantilevered truss to be about .0045. The damping ratio will decrease when large bodies are added to the truss. In the absence of air, the damping can be expected to be even smaller, perhaps approaching .002.

Past practices of using a constant damping ratio of .005 for Space Station studies does not represent the worst case. Lower values of damping should be used which reflect mass loading and internal loading effects.

CONCLUDING REMARKS

The Mini-MAST truss has been tested and analyzed for the purpose of understanding the dynamic characteristics, nonlinear stiffness and hysteretic damping of large spacecraft.

It was necessary to use a Timoshenko beam model for bending to account for the shear deformation of the Mini-MAST truss. The modal frequencies of the Euler beam model were higher than the actual values.

A tangent function model of the nonlinear torsional stiffness was developed and its parameters estimated to match experimental results.

A hysteretic slip model for torsion was developed using the experimental test data. The slip distribution function used has a second order, exponential form. The hysteretic behavior is expected to be affected by changes in the vertical loading due to gravity.

The damping contribution in torsion of the hysteretic behavior was deduced by analyzing the torsional slip model. The damping due to slipping was determined to be quite dependent on loading conditions. A steady load, for example, might eliminate slipping and consequently any damping contribution due to slipping.

Future studies of control system performance should use lower values of structural damping than the .005 used in the past, and should consider the nonlinear effects.

REFERENCES

1. Young, John W. and Frederick J. Lallman: Control/Structures Interaction Study of Two 300 KW Dual-Keel Space Station Concepts. NASA Technical Memorandum 87679. May 1986.

2. Adams, Louis R.: Design, Development and Fabrication of a Deployable/Retractable Truss Beam Model for Large Space Structures Application. NASA Contractor Report 178287. June 1987.

3. Taylor, Lawrence W., Jr.: On-Orbit Systems Identification of Flexible Spacecraft. 7th IFAC Symposium on Identification and System Parameter Estimation. York, England. July 2-8, 1985.

4. Noor, A. K., Anderson, M. S. Anderson and W. H. Greene: Continuum Models for Beam- and Platelike lattice Structures. AIAA J., v. 16, no. 12, December 1978.

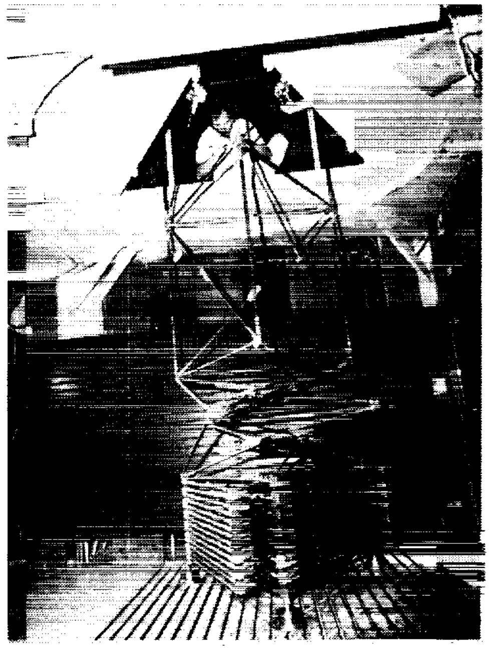

Figure 1a. The Mini-MAST Truss Being Deployed.

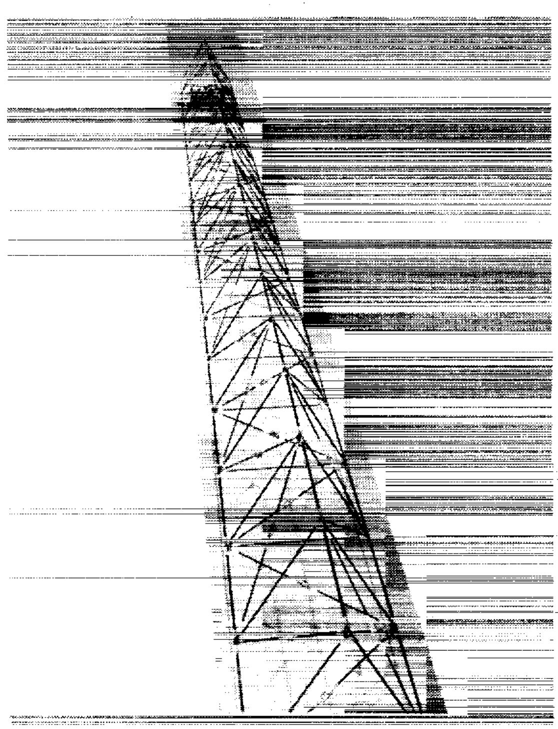

Figure 1b. The Mini-MAST Truss Fully Deployed.

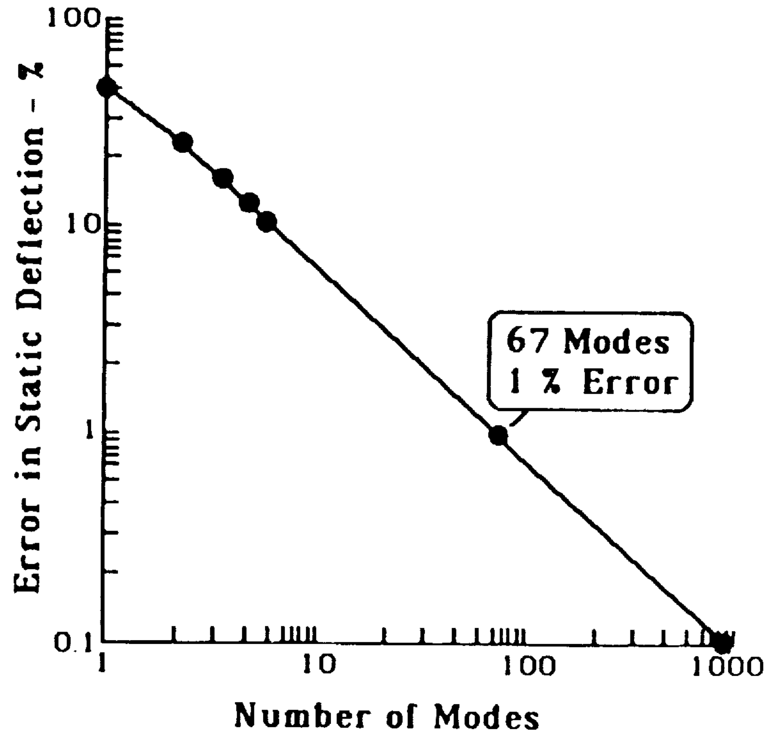

Figure 2. The Number of Modes Required for a Modal Model to Accurately Represent the Static Deflection of a Cantilevered Euler Beam.

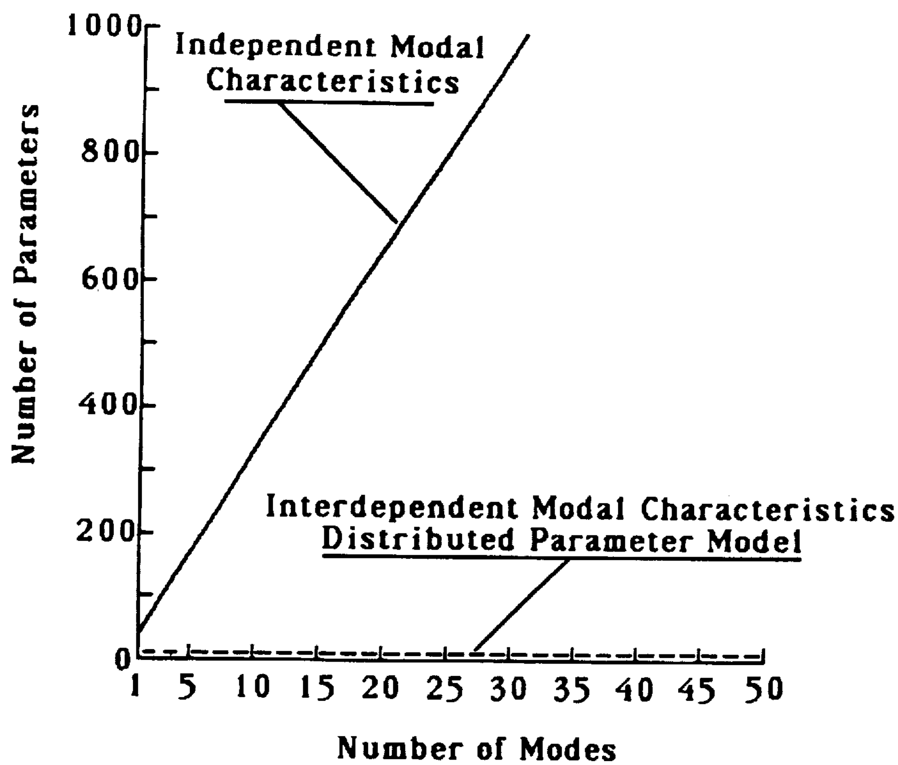

Figure 3. Comparison of the Number of Model Parameters for Modal Models and Distributed Parameter Models.

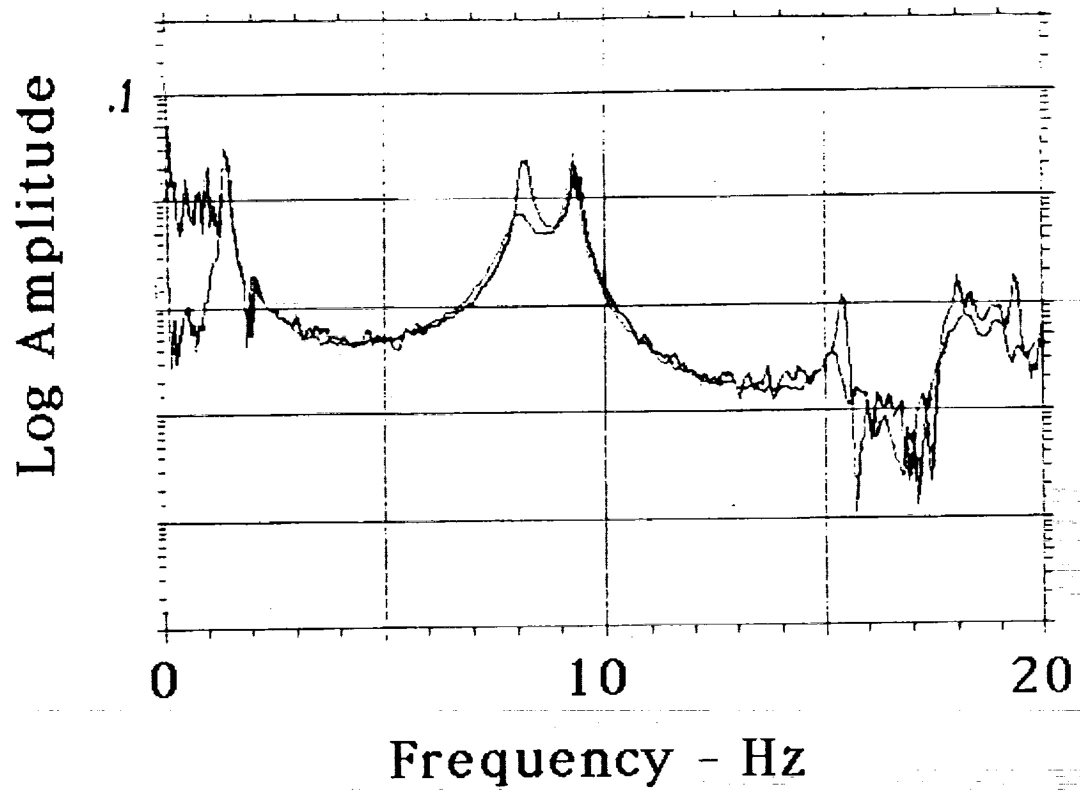

Figure 4a. Frequency Response of the Mini-MAST Truss in Term of Inches of Response per Pound of Input. Frequency from 0 to 20 Hz.

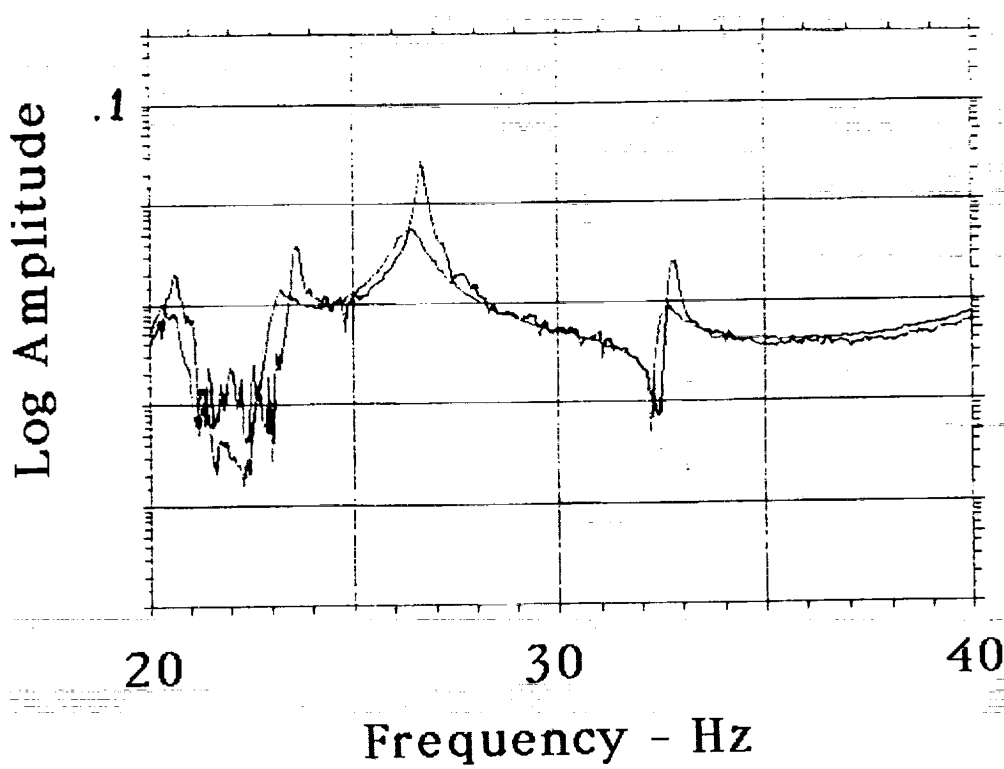

Figure 4b. Frequency Response of the Mini-MAST Truss in Term of Inches of Response per Pound of Input. Frequency from 20 to 40 Hz.

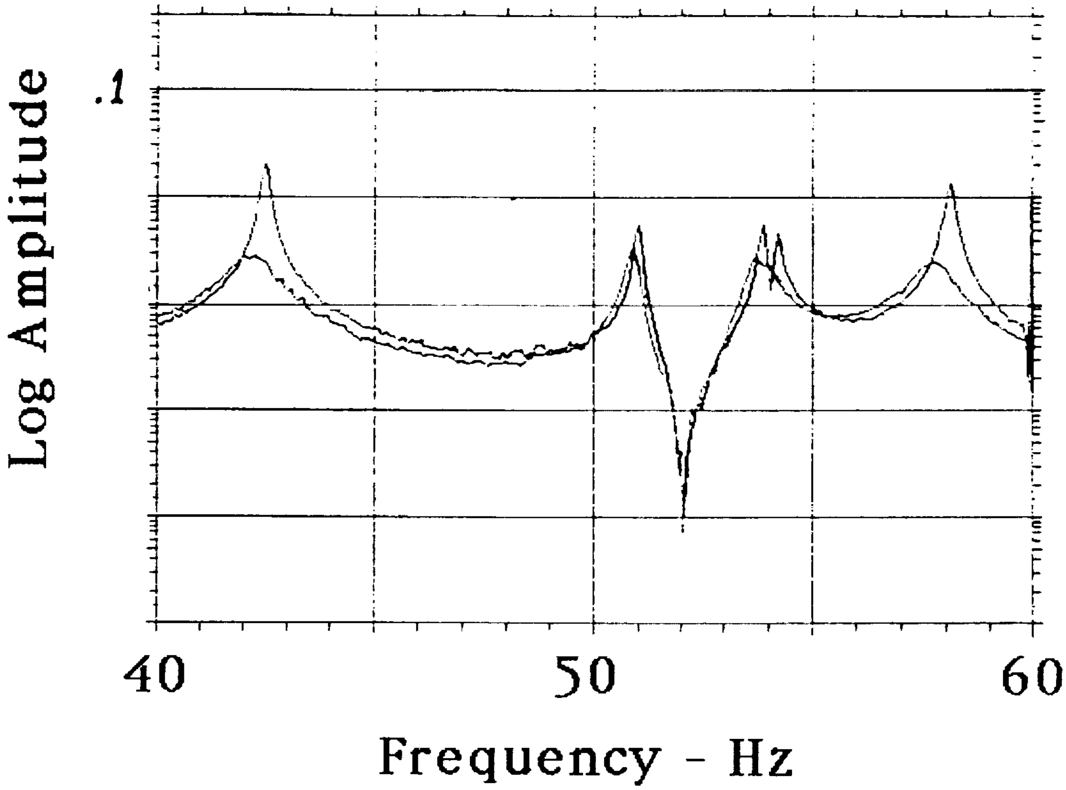

Figure 4c. Frequency Response of the Mini-MAST Truss in Term of Inches of Response per Pound of Input. Frequency from 40 to 60 Hz.

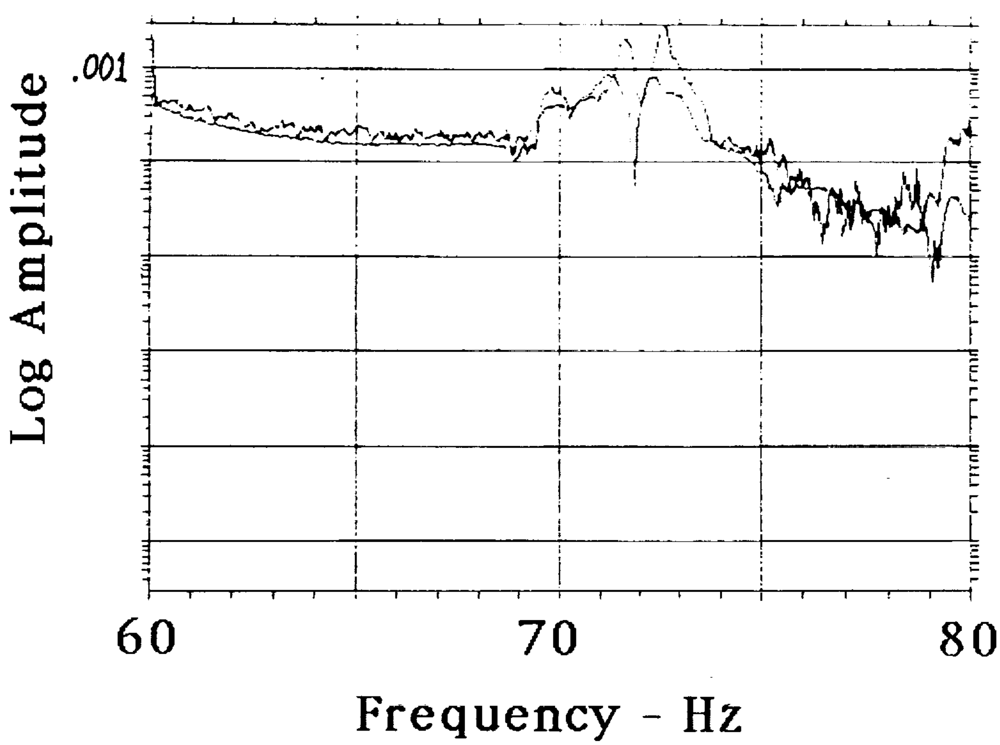

Figure 4d. Frequency Response of the Mini-MAST Truss in Terms of Inches of Response per Pound of Input. Frequency from 60 to 80 Hz.

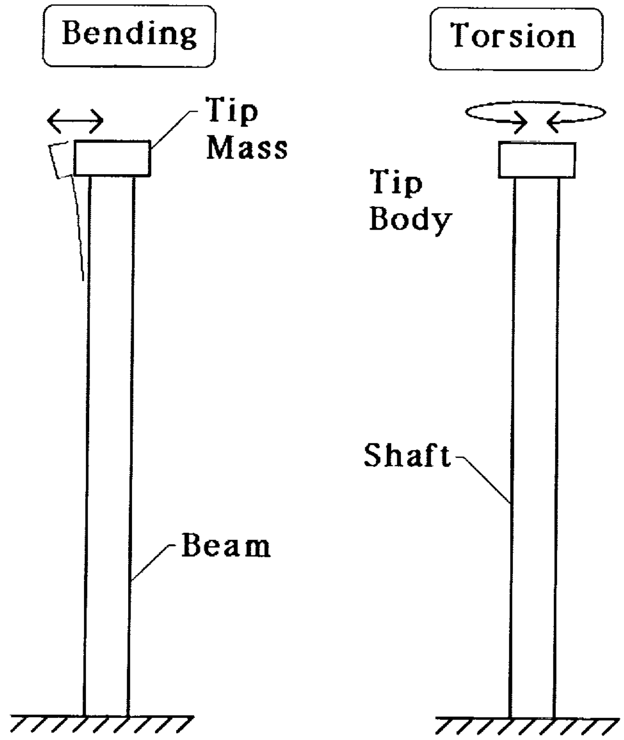

Figure 5. Schematics of Distributed Parameter Models for Bending and Torsion.

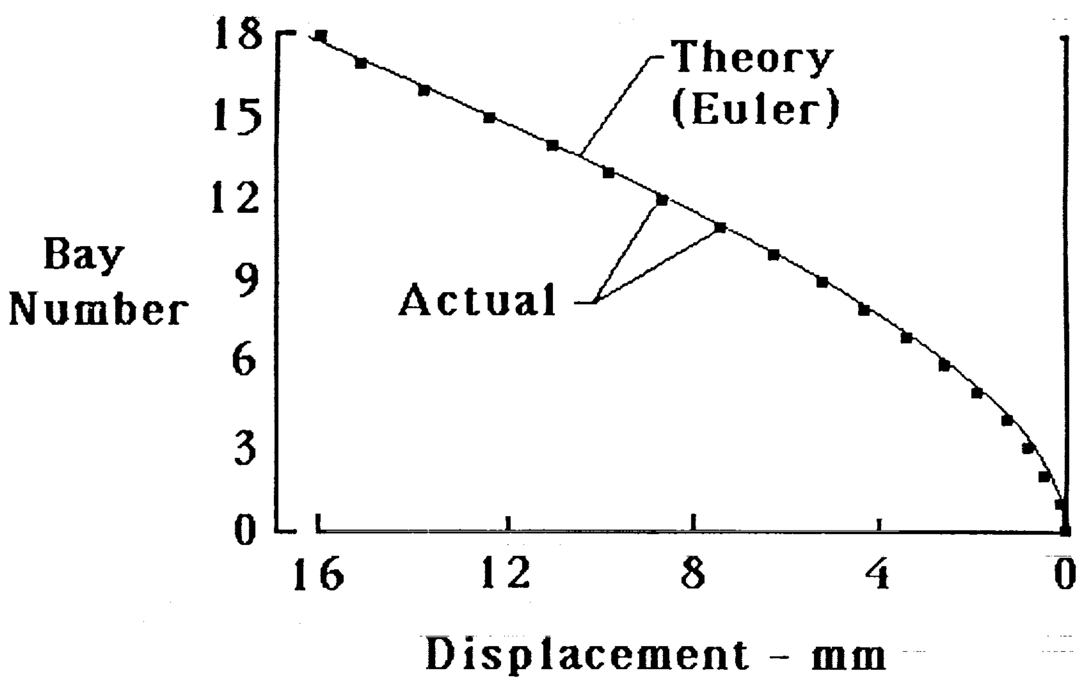

Figure 6. Comparison of the Model and Actual Static Deflection in Bending of the Mini-MAST Truss Subjected to a 15 Pound Force at the Top.

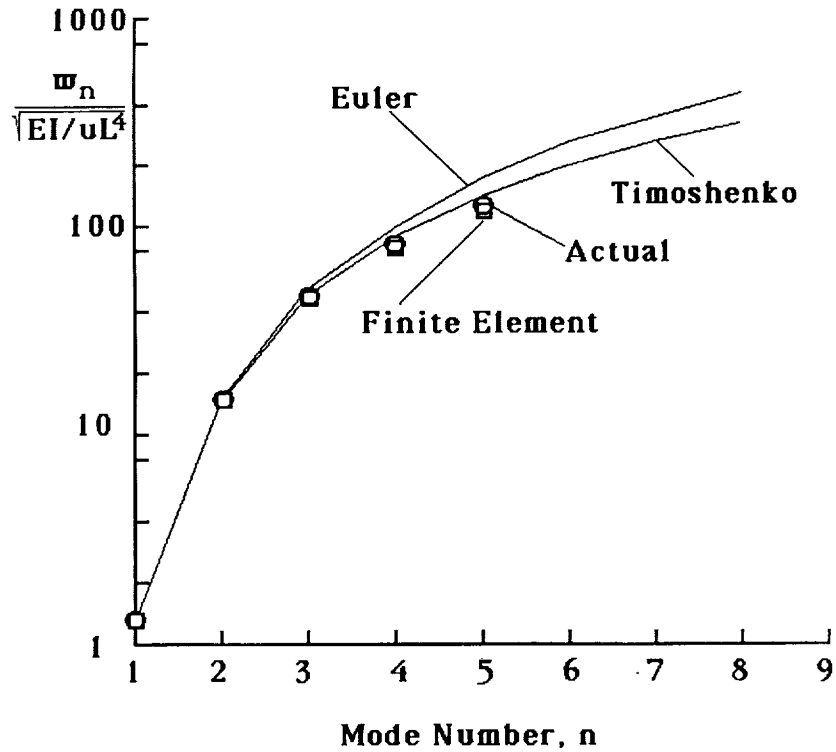

Figure 7. Comparison of Distributed Parameter Model, Finite Element Model and Actual Normalized Bending Frequencies.

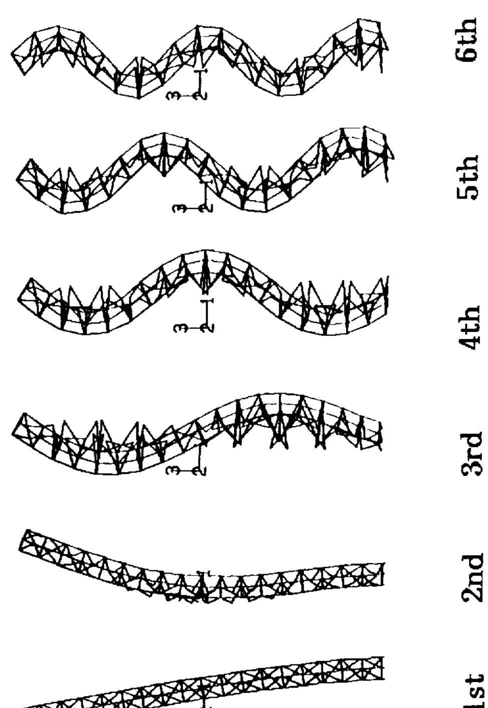

Figure 8. Finite Element Model Mode Shapes for Bending.

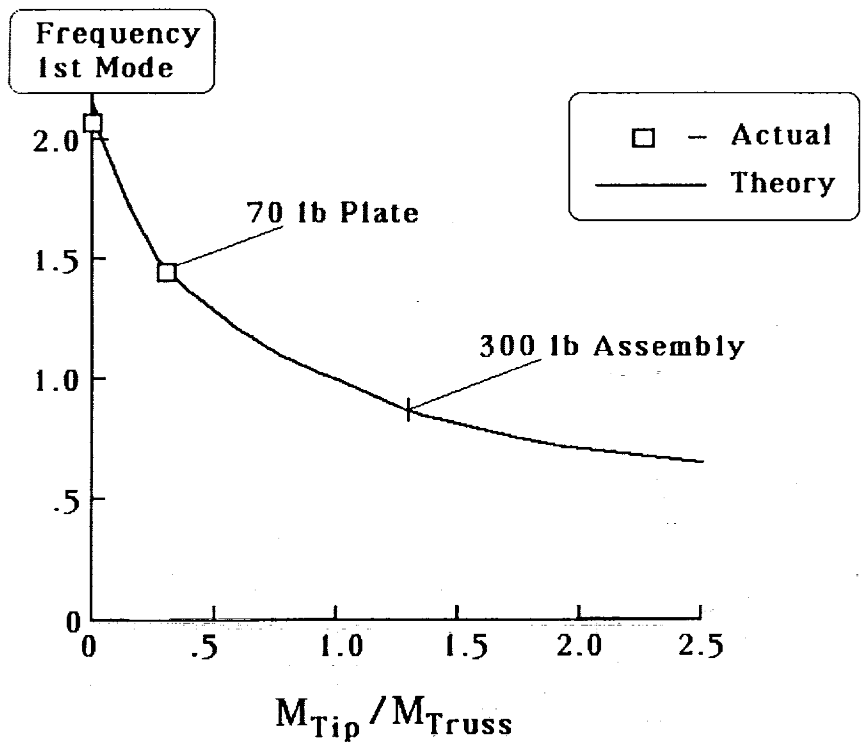

Figure 9. Comparison of the Model and Actual First Mode Bending Frequencies as a Function of Tip Mass to Truss Mass Ratio.

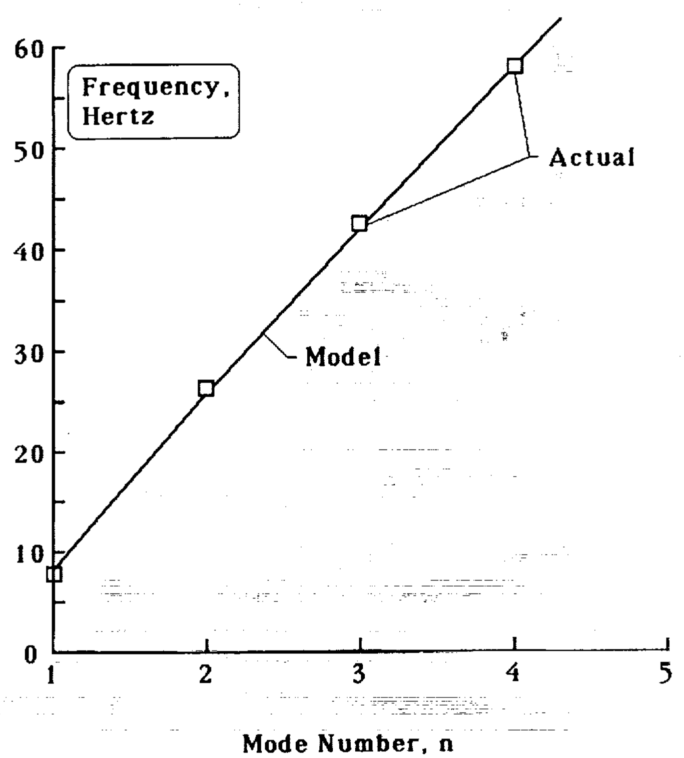

Figure 10. Comparison of Model and Actual Torsion Mode Frequencies.

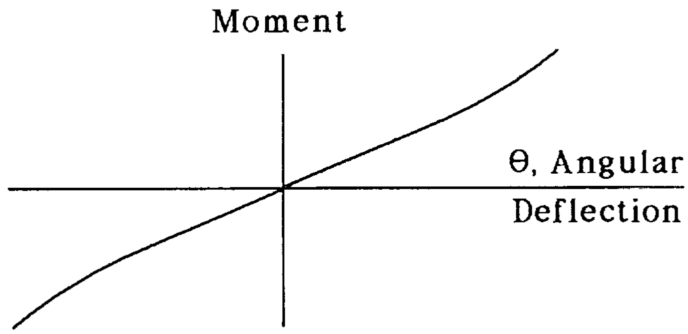

$$M = \frac{K}{B}\mathrm{Tan}(B\theta) \quad \text{or} \quad \theta = \frac{1}{B}\mathrm{Arctan}\left(\frac{MB}{K}\right)$$

$$\underbrace{\left.\frac{d\theta}{dM}\right|_{M=0} = \frac{1}{K}}_{\text{Linear}} \qquad \underbrace{\left.\frac{d^3\theta}{dM^3}\right|_{M=0} = \frac{2B^2}{K^3}}_{\text{Cubic}}$$

Figure 11. Nonlinear Stiffness Formulation Used for the Torsion Model.

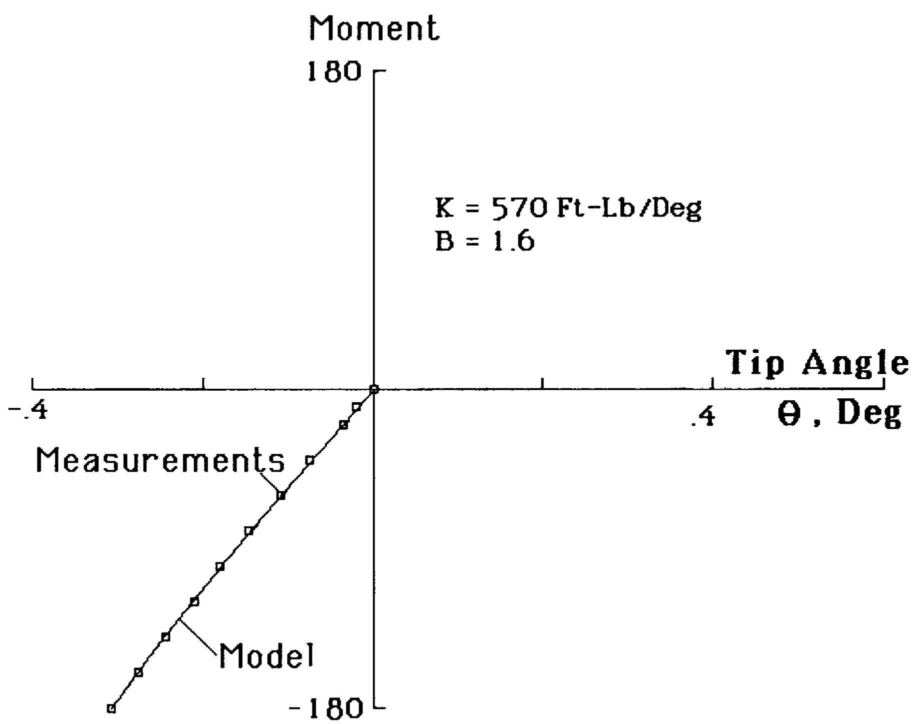

Figure 12. Comparison of Model and Actual Static Deflection in Torsion.

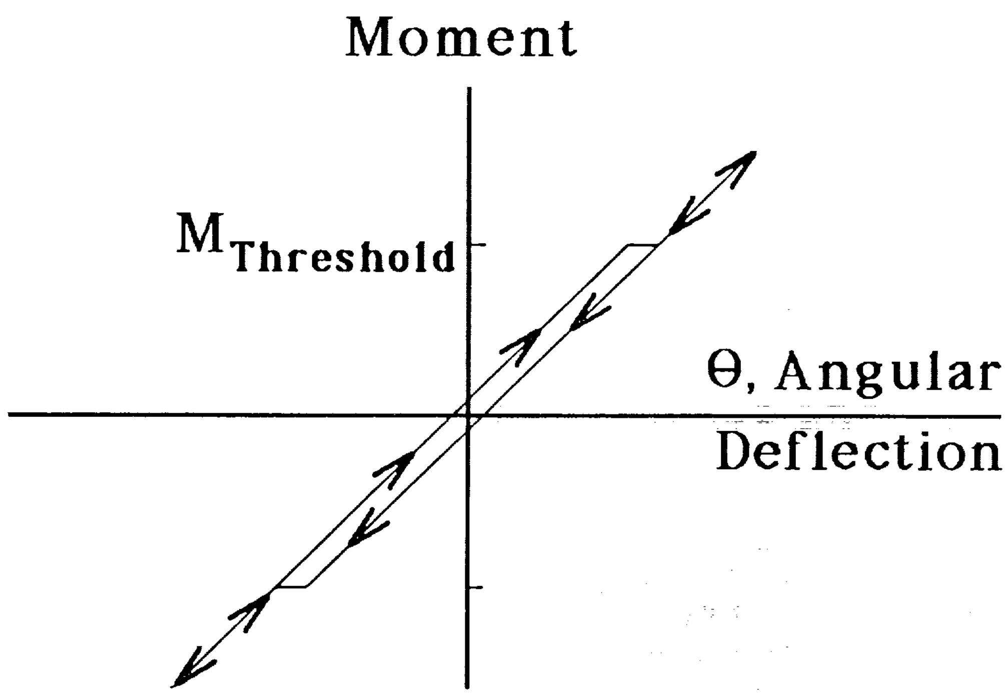

Figure 13. An Individual Nonlinear Slip Element for the Torsion Model.

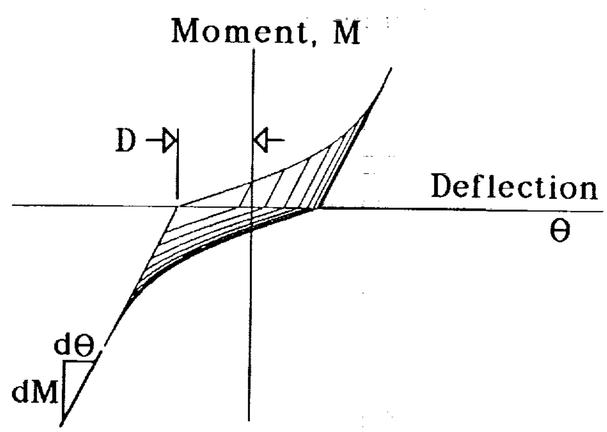

$$\theta = M/K + D\int_{A}^{M} P'(M)\,dM$$

$$A = M_{reversal} \quad \text{if} \quad M_{reversal} > 0$$

$$= 0 \quad \text{if} \quad M_{reversal} < 0$$

Figure 14. Nonlinear Hysteretic Model for Torsion.

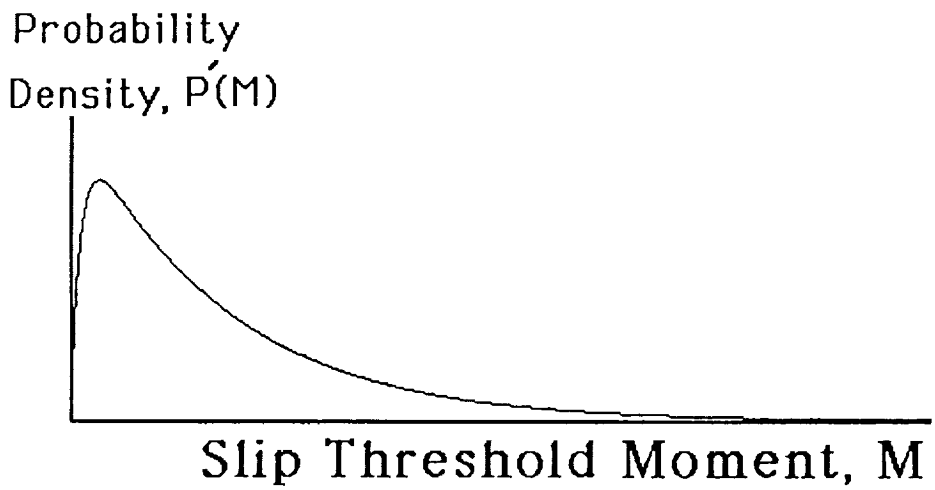

$$P'(M) = -\frac{e^{-M/X1}}{X2-X1} + \frac{e^{-M/X2}}{X2-X1}$$

Figure 15. The Slip Distribution Function.

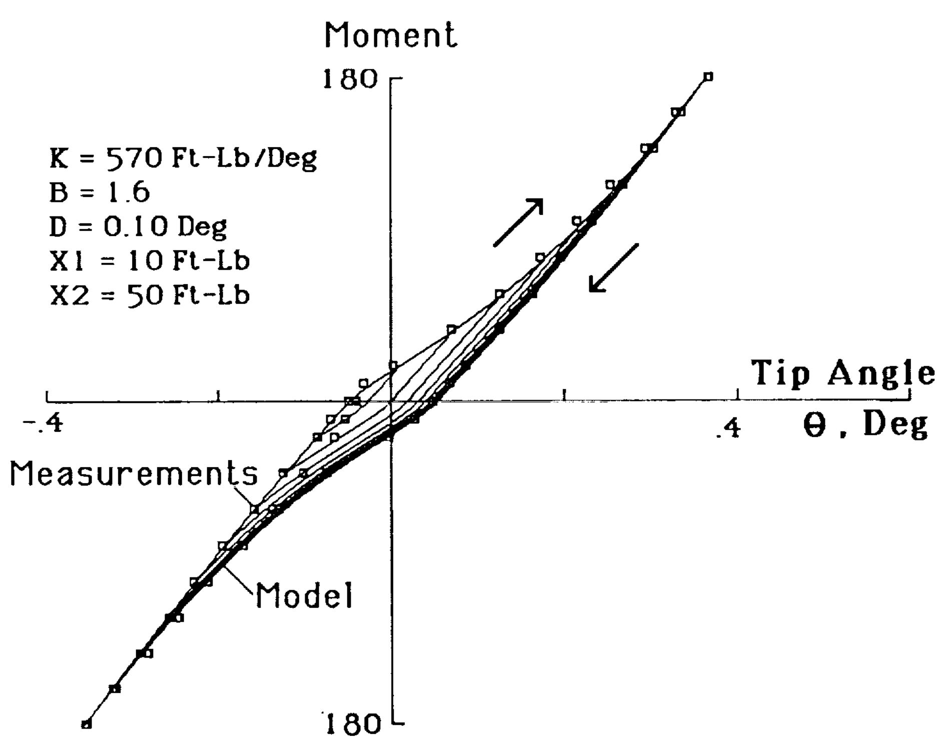

Figure 16. Comparison of Hysteretic Model and Actual Static Deflection in Torsion.

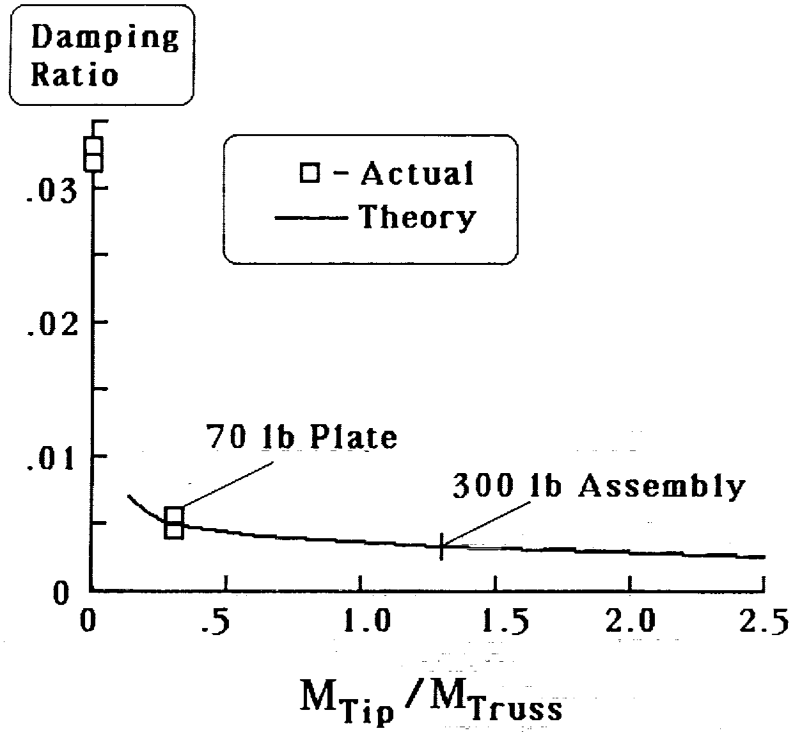

Figure 17. Comparison of Model and Actual Damping Ratios in Bending as a Function of Tip Mass to Truss Mass Ratio.

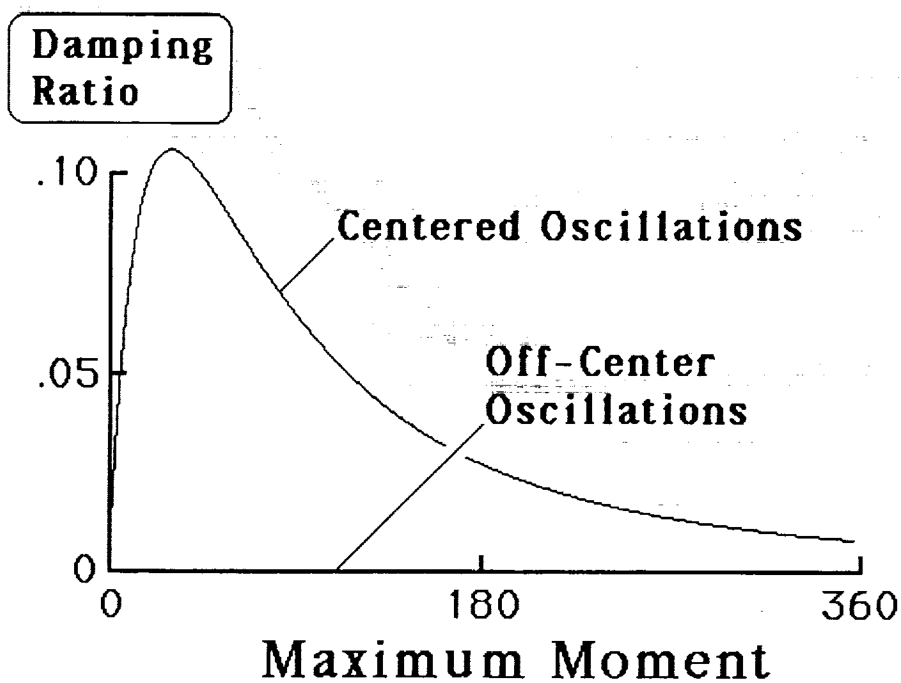

Figure 18. Effect of the Hysteretic Behavior on Damping in Torsion.